

Structural and magnetic properties of $\text{Gd}_5\text{Si}_x\text{Sn}_{4-x}$

H. B. Wang, Z. Altounian, and D. H. Ryan

Physics Department and Centre for the Physics of Materials, McGill University, 3600 University Street, Montreal, Quebec, Canada H3A 2T8

(Received 5 September 2002; published 18 December 2002)

The ternary $\text{Gd}_5\text{Si}_x\text{Sn}_{4-x}$ alloy system has been shown to exist for all x . Structural and magnetic phase diagrams have been derived. Si-rich and Sn-rich alloys are orthorhombic and order ferromagnetically, with T_c increasing with Si content. Intermediate compositions are monoclinic, and exhibit a disordered noncollinear magnetic order. In the ordered state, ^{119}Sn Mössbauer spectroscopy shows transferred hyperfine fields approaching 37 T at Sn sites in the orthorhombic form, and severely broadened spectra with much smaller fields in the monoclinic form. For $x \leq 0.4$, there is, on heating, a first-order magnetic and structural transition from a ferromagnetic to a nonmagnetic state that may be associated with a giant magnetocaloric effect.

DOI: 10.1103/PhysRevB.66.214413

PACS number(s): 75.30.Sg, 76.80.+y, 75.50.Cc

I. INTRODUCTION

The structures of Gd_5Si_4 and Gd_5Ge_4 were reported by Smith *et al.*,¹ while some structural and magnetic properties of the ternary $\text{Gd}_5\text{Si}_{4-x}\text{Ge}_x$ compounds were reported by Holtzberg *et al.*² Interest in these compounds was rekindled recently by the discovery of the giant magnetocaloric effect in $\text{Gd}_5\text{Si}_2\text{Ge}_2$,³ suggesting potential applications in magnetic refrigeration. The structural phase diagram⁴ and a zero-field magnetic phase diagram⁵ for $\text{Gd}_5\text{Si}_x\text{Ge}_{4-x}$ were soon published. 5:4 ternary compounds with other rare earths have also been investigated.⁶⁻⁸ The magnitude of the magnetocaloric effect in these compounds is a consequence of the magnetic transition being first order. In the $\text{Gd}_5\text{Si}_x\text{Ge}_{4-x}$ giant magnetocaloric materials, the magnetic transition is accompanied by, or possibly driven by, a structural phase transition.⁹ It is crucial therefore to determine the structural as well as magnetic phase diagrams for these compounds. In this paper, we report the results of such a study for $\text{Gd}_5\text{Si}_x\text{Sn}_{4-x}$. Our motivation was twofold. First, if ternary 5:4 compounds containing Sn can be formed across the full composition range, one may be able to extend the temperature range over which the giant magnetocaloric effect occurs. Second, as Gd-containing compounds are not readily studied by neutron diffraction, detailed magnetic characterization is impeded. With Sn in the structure, one can use ^{119}Sn Mössbauer spectroscopy. In this way, the magnetic and chemical environment of each crystallographically inequivalent Sn atom can be investigated.

II. EXPERIMENTAL METHODS

Samples were prepared in a tri-arc furnace with a base pressure of better than 6×10^{-7} mbar. Stoichiometric amounts of the pure elements [Gd (99.9%) Si (99.9999%) and Sn (99.99%)] were melted several times under pure (less than 1 ppm impurity) argon to ensure homogeneity. The tin-rich alloys were air sensitive, tending to segregate into metallic tin and gadolinium oxide on exposure to air for a few hours. All sample handling was therefore performed under argon in a glove box.

Powder x-ray-diffraction measurements were made using

Cu K_α radiation. The sample was ground under argon in the glove box and then transferred to an evacuated enclosure with a kapton window for the measurements. Diffraction patterns were analyzed using GSAS (Ref. 10) to extract lattice parameters. Atomic locations were taken from Gd_5Si_4 (Ref. 4) for the orthorhombic phases, and from $\text{Gd}_5\text{Si}_2\text{Ge}_2$ (Ref. 4) for the monoclinic phase, and were not refined.

Basic magnetic characterization was carried out on a commercial susceptometer/magnetometer at temperatures from 5 K to room temperature (RT). ac susceptibility (χ_{ac}) measurements were made with a driving field of 1 mT at 137 Hz. Magnetization measurements were made in fields of up to 6 T.

Mössbauer measurements were obtained on a constant-acceleration spectrometer using a 74-MBq ^{119m}Sn BaSnO_3 source. Temperatures between 12 K and room temperature were achieved using a vibration-isolated closed-cycle refrigerator. The spectra were fitted using a conventional nonlinear least-squares minimization routine that allowed for both Lorentzian lines from sharp components and Gaussian field distributions from disordered components. The spectrometer was calibrated against a 99.99% α -Fe foil using a ^{57}Co source mounted on the back of the drive. Typical linewidths for the ^{119}Sn spectra were 0.44 mm/s (full width at half maximum).

III. STRUCTURAL CHARACTERIZATION

Analysis of the Cu K_α x-ray-diffraction patterns (Fig. 1) shows that the phase behavior of $\text{Gd}_5\text{Si}_x\text{Sn}_{4-x}$ is somewhat similar to that of the $\text{Gd}_5\text{Si}_x\text{Ge}_{4-x}$ alloy system.⁴ Gd_5Sn_4 adopts the orthorhombic $Pnma$ Sm_5Sn_4 -type structure (no. 62), and this form is observed for compounds with $x \geq 2.8$ and $x \leq 0.4$. Lattice parameters obtained from the GSAS fits are listed in Table I. For compositions in the range $0.8 \leq x \leq 1.2$, the alloys adopt the monoclinic $P112_1/a$ $\text{Gd}_4\text{Si}_2\text{Ge}_2$ -type structure (no. 14) previously reported in the $\text{Gd}_5\text{Si}_x\text{Ge}_{4-x}$ system.⁴ In the center of the phase diagram ($1.6 \leq x \leq 2.4$) the alloys consistently crystallize as a two-phase mixture of orthorhombic and monoclinic forms, with the orthorhombic fraction increasing with x . This two-phase assignment was confirmed by ^{119}Sn Mössbauer spectroscopy.

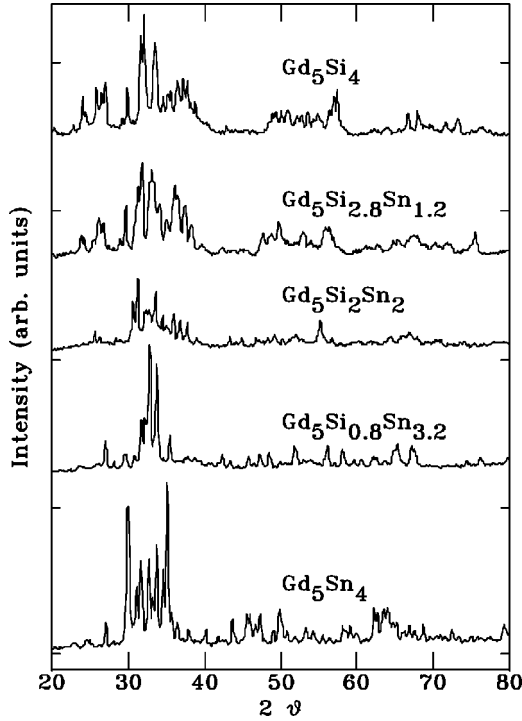


FIG. 1. Typical Cu K_α diffraction patterns for $Gd_4Si_xSn_{4-x}$.

copy, and the phase fractions derived from both Mössbauer spectroscopy and the GSAS analysis of the Cu K_α x-ray-diffraction patterns are summarized in Fig. 2. The agreement between the two techniques is excellent, however, the Mössbauer data suggest that the two-phase region extends all the way to $x=3.6$ with $\sim 5-10\%$ of the monoclinic form being seen in the Mössbauer spectra, but not detected in the x-ray-diffraction patterns. The situation for $x \leq 0.8$ is more complex and is discussed later.

The orthorhombic Sm_5Sn_4 -type structure has three metalloid sites: $4c_1$, $4c_2$, and $8d$, and three rare-earth sites: $4c$,

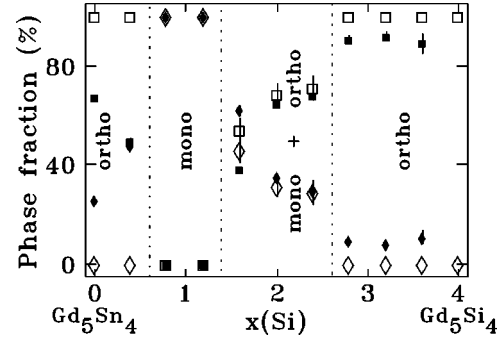


FIG. 2. Comparison of phase fractions derived from GSAS analysis of room-temperature Cu K_α diffraction patterns (open symbols) and 12-K ^{119}Sn Mössbauer spectroscopy (solid symbols). The structural boundaries are shown as dotted lines. Note the excellent agreement in the monoclinic (\diamond) and orthorhombic (\square) fractions derived from the two techniques for $x > 0.8$. The discrepancies for $x \leq 0.8$ are related to a first-order structural change that occurs at low temperatures.

$8d_1$, and $8d_2$. The metalloid (Sn for the purposes of this discussion) sites divide into two groups. Sn atoms at the $4c_2$ and $8d$ sites have seven Gd nearest neighbors compared to eight Gd atoms for Sn($4c_1$). Furthermore, if we restrict our attention to those neighbors close enough to be in effective contact, then Sn atoms at the $4c_2$ and $8d$ sites have five Gd neighbors compared to four for Sn($4c_1$). We therefore anticipate two distinct sites in the Mössbauer spectra with slightly ($\sim 20\%$) different hyperfine fields. The monoclinic form appears to exhibit significant levels of disorder as the ^{119}Sn Mössbauer spectra are extremely broad and exhibited greatly reduced hyperfine fields. This feature made the monoclinic form easy to distinguish from the orthorhombic phase in the Mössbauer spectra, and assisted in mapping out the orthorhombic-monoclinic coexistence region shown in Fig. 2.

TABLE I. Structural parameters for $Gd_4Si_xSn_{4-x}$ obtained by GSAS refinement of Cu K_α diffraction patterns. For $1.6 \leq x \leq 2.4$ two crystal forms were found to be present.

Composition	Structure	a (Å)	b (Å)	c (Å)	V (Å ³)	γ (°)
Gd_5Sn_4	$Pnma$	8.047(3)	15.545(5)	8.199(3)	1025.7(8)	90
$Gd_5Si_{0.4}Sn_{3.6}$	$Pnma$	7.954(5)	15.491(9)	8.188(5)	1008.9(8)	90
$Gd_5Si_{0.8}Sn_{3.2}$	$P112_1/a$	7.252(5)	14.638(8)	8.096(5)	857.6(7)	93.81(7)
$Gd_5Si_{1.2}Sn_{2.8}$	$P112_1/a$	7.225(5)	14.625(8)	8.063(5)	850.5(7)	93.41(6)
$Gd_5Si_{1.6}Sn_{2.4}$	$P112_1/a$	7.155(5)	14.551(11)	8.030(6)	834.9(13)	92.97(5)
	$Pnma$	7.708(5)	15.280(12)	8.073(5)	950.8(16)	90
$Gd_5Si_2Sn_2$	$P112_1/a$	7.115(5)	14.481(12)	7.870(7)	810.4(13)	92.08(6)
	$Pnma$	7.662(4)	15.144(7)	8.013(4)	929.8(11)	90
$Gd_5Si_{2.4}Sn_{1.6}$	$P112_1/a$	7.105(5)	14.423(9)	7.844(5)	803.6(8)	91.39(5)
	$Pnma$	7.610(2)	15.045(5)	7.963(2)	911.8(7)	90
$Gd_5Si_{2.8}Sn_{1.2}$	$Pnma$	7.576(5)	14.956(10)	7.926(6)	898.0(16)	90
$Gd_5Si_{3.2}Sn_{0.8}$	$Pnma$	7.525(4)	14.858(8)	7.839(4)	876.5(12)	90
$Gd_5Si_{3.6}Sn_{0.4}$	$Pnma$	7.486(3)	14.797(5)	7.805(3)	864.6(4)	90
Gd_5Si_4	$Pnma$	7.480(5)	14.734(10)	7.743(5)	853.3(14)	90

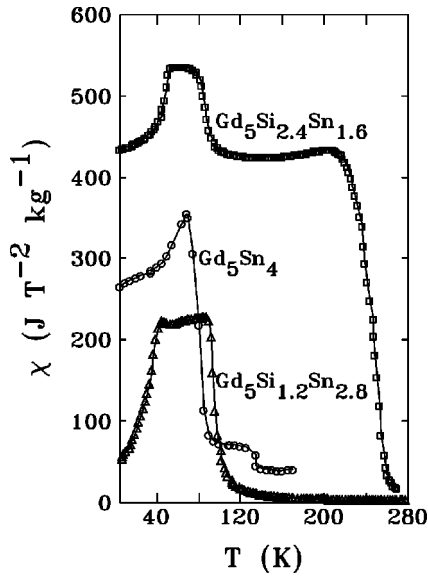


FIG. 3. Typical χ_{ac} vs T data showing the large susceptibility observed below the ordering temperatures and the overall decline in ordering temperature with increasing Sn content in $\text{Gd}_5\text{Si}_x\text{Sn}_{4-x}$. Both the $x=0$ and $x=2.4$ samples show two ordering events, the latter due to the presence of two magnetic phases, the former resulting from a structural transition at ~ 85 K.

IV. BASIC MAGNETIC BEHAVIOR

χ_{ac} measurements gave large signals below the ordering temperature of each alloy, suggesting ferromagnetic ordering of the gadolinium moments across the whole composition range (Fig. 3). χ_{ac} vs temperature reveals a single sharp transition for $x \leq 1.2$ and $x > 2.4$ with evidence for two distinct transitions for $1.6 \leq x \leq 2.4$, consistent with the second phase detected by x-ray diffraction. As has been previously reported for Ge substitution in $\text{Gd}_5\text{Si}_x\text{Ge}_{4-x}$,⁵ the replacement of Si by Sn leads to a steady reduction in the ordering temperature of the orthorhombic $\text{Gd}_5\text{Si}_x\text{Sn}_{4-x}$ alloys. By contrast, the transition temperature of the monoclinic form in this system appears essentially independent of Sn content at ~ 100 K, and may actually fall slightly as the average Si content of the alloy is increased. The transition temperatures identified by χ_{ac} are summarized in Fig. 4.

The binary Gd_5Sn_4 alloy also exhibits two, well separated, magnetic transitions, despite appearing to be single-phased by x-ray diffraction. The upper event (Fig. 3) is much weaker, and might easily be assigned to an impurity. However, the likeliest magnetic impurity is Gd_5Sn_3 , and as this orders ~ 75 K,¹¹ it would have to be the majority phase present in order to account for the ~ 80 K event in Fig. 3. This is inconsistent with both the x-ray-diffraction data and the ^{119}Sn Mössbauer spectra presented below. As we will show, both features are intrinsic to the material and the lower feature in the $\chi_{ac}(T)$ data is in fact associated with a first-order structural and magnetic transition.

High-field magnetization measurements at 5 K generally yielded conventional ferromagnetic behavior with large saturation moments consistent with collinear ordering of the Gd. Values obtained by extrapolating to infinite field vs $1/B$ are

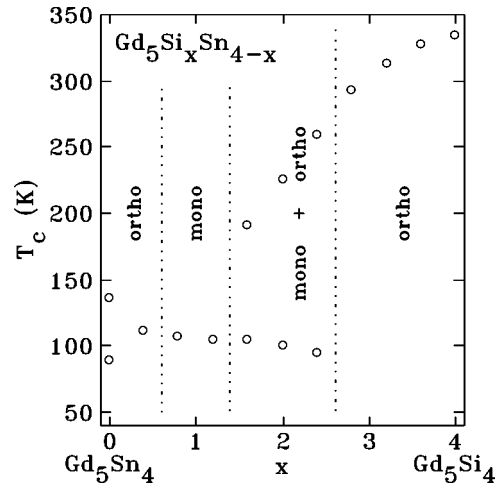


FIG. 4. Magnetic phase diagram for $\text{Gd}_5\text{Si}_x\text{Sn}_{4-x}$ deduced from $\chi_{ac}(T)$ data. Note the presence of two magnetic phases around $x=2$ and also at $x=0$. The structural boundaries derived from x-ray diffraction are also shown as dotted lines.

shown in Fig. 5. This procedure was adopted because of the severe curvature around $x=1$, and yielded values approximately $0.2-0.5\mu_B/\text{Gd}$ larger than extrapolating to zero field in the single-phased regions. The magnetization around $x=1$ is greatly reduced, and the curves did not saturate, indicating that the monoclinic phase present at these compositions has a more complex magnetic structure that is likely noncollinear. The monoclinic phase is also present at significant, but decreasing, concentrations from $x=1.6$ to $x=2.4$ (Fig. 2) and the slowly increasing magnetization apparent in Fig. 5 reflect the increasing volume fraction of the more strongly magnetic orthorhombic phase.

V. ^{119}Sn MÖSSBAUER RESULTS

The spectrum of Gd_5Sn_4 at 12 K (Fig. 6) is dominated by two well-split magnetic sextets that account for about 70% of the total absorbed area. In addition, there is a singlet with an isomer shift of $+2.4$ mm/s. With these primary features subtracted, there is an additional component visible, that could be fitted as the sum of two Gaussian distributions of hyperfine fields, and which accounts for about 25% of the total area. These three basic components were present to

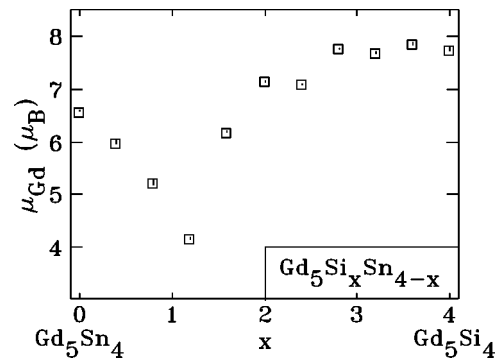


FIG. 5. Magnetization extrapolated to $1/B=0$ as a function of composition in $\text{Gd}_5\text{Si}_x\text{Sn}_{4-x}$ at 5 K.

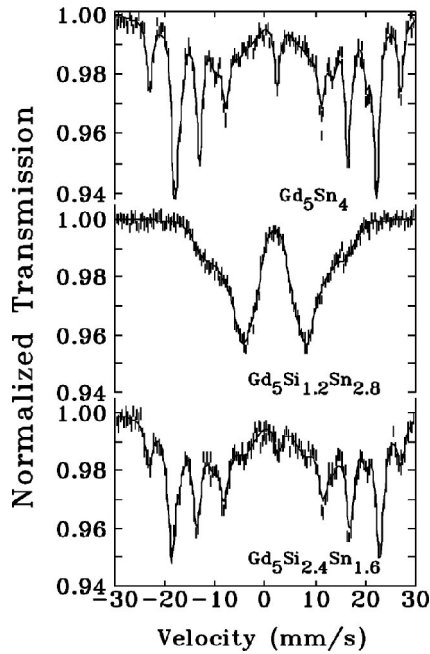


FIG. 6. ^{119}Sn Mössbauer spectra of three $\text{Gd}_5\text{Si}_x\text{Sn}_{4-x}$ samples at 12 K. The two sharp sextets and the singlet components are clearly visible in the $x=0$ and $x=2.4$ spectra, while the $x=1.2$ spectrum shows the two distinct Gaussian distributions.

varying degrees in the spectra of the whole series. The exceptions were again at $x=0.8$ and 1.2 , where only the Gaussian distributions were observed. The two Gaussian-broadened subcomponents are clearly visible in the spectrum of $\text{Gd}_5\text{Si}_{1.2}\text{Sn}_{2.8}$ at 12 K shown in Fig. 6. The extremely broad distribution of hyperfine fields ($\sigma_{B_{hf}}=3$ T) observed for this component (reminiscent of many metallic glasses) is a clear indication that the monoclinic phase that occurs in this composition range is highly disordered, confirming the conjecture made on the basis of the x-ray data. Furthermore, the greatly reduced hyperfine fields for the two broad components suggests that the Gd moments are ordered noncollinearly so that their transferred fields do not add coherently at the Sn sites. This is fully consistent with the reduced magnetization observed for the monoclinic phase (Fig. 5).

The relative areas of the three components are plotted as a function of composition in Fig. 7. The sharp component accounts for $\sim 90\%$ of the area for $x>2.4$, however, as more tin is added, the Gaussian sextets become more prominent. They are the only feature observed for $x\sim 1$ but the sharp component returns as $x\rightarrow 0$. We therefore associate the sharp components with the orthorhombic structure observed by x-ray diffraction at the Sn-rich and Sn-poor ends of the alloy series, and the broad components with the disordered monoclinic structure seen near $x=1$. It is interesting to note that a broad contribution with an average field of about 10 T was also present in Gd_5Sn_3 at 4.2 K,¹¹ suggesting that disordered structures are not uncommon in the Gd-Sn system. We will return to the apparently multiphase nature of the Gd_5Sn_4 alloy later.

The hyperfine fields at the tin in the two sharp sextets are remarkably large, being 29.4 and 36.6 T at 12 K for $x=0$.

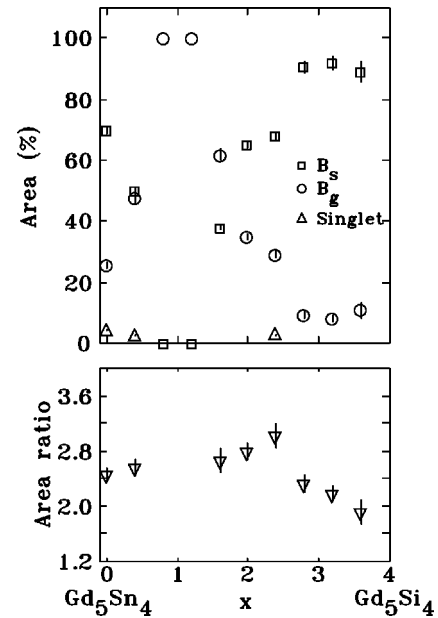


FIG. 7. Top: Relative areas of the three components observed in the spectra at 12 K. B_s is the combined areas of the two sharp sextets, B_g shows the total area of the Gaussian broadened sextets and the triangles give the area of the singlet. Bottom: Area ratio of the low- and high-field sextets that make up the sharp, magnetically split component of the spectra.

These fields are both larger than the 28 T reported for Gd_5Sn_3 ,¹¹ and this helps rule out the presence of Gd_5Sn_3 as a significant impurity. The area ratio for the two sites is 2.5:1, a rather poor match for the 3:1 expected from the $(4c_2+8d):(4c_1)$ pairing derived from the structural analysis above. However, the field ratio (1.24:1) is very close to the 5:4 expected when the nearest Gd neighbors were counted. Despite the factor of three decline in ordering temperature with increasing tin content, the hyperfine fields at the two tin sites in the orthorhombic form are essentially composition independent. The larger field does not change, while the lower field declines slightly from ~ 31 T at $x\sim 4$ to ~ 29 T by $x=0$ (Fig. 8). This is consistent with the magnetization data that show ferromagnetic ordering of the full Gd moment across the whole composition range. The relative areas of the two sharp components are not constant, and the area of the 30-T component ranges from two to three times that of the 36-T component (lower panel of Fig. 7). This behavior likely reflects some preferential site occupation by the Sn atoms.

The high-field component of the two Gaussian broadened sextets exhibits a composition independent field of ~ 20 T, while the lower field component is more variable, passing through a broad minimum around $x=0.8$ where the Gaussian sextets are dominant. As with the sharp sextets, it is the lower field component that has the larger area, however, the area ratio is not so large, being only 1.7:1. The average hyperfine field in this broadened component at $x=1.2$ is 14.1 T, less than half that seen in the sharp sextet pattern, consistent with the greatly reduced magnetization of this disordered phase (Fig. 5) and suggesting that the magnetic ordering of the Gd moments is noncollinear.

Figure 9 shows the temperature dependence of the spectra

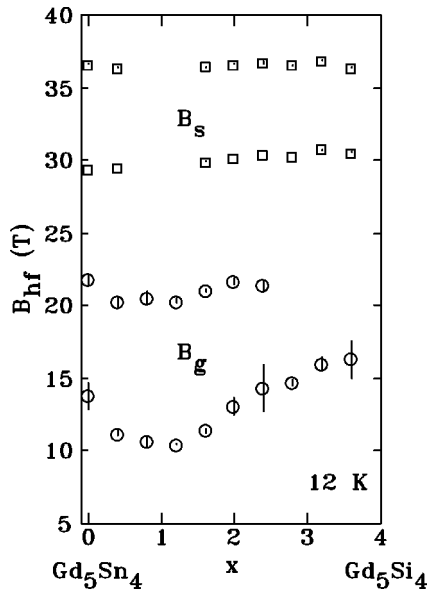


FIG. 8. Composition dependence of the hyperfine fields observed for the sharp (B_s) and Gaussian-broadened (B_g) components at 12 K. For $x=0.8$ and 1.2 only the Gaussian components were observed, while for $x>2.4$ the Gaussian component was too weak to permit the two components to be distinguished.

for $\text{Gd}_5\text{Si}_{1.2}\text{Sn}_{2.8}$. This material exhibits several unusual features. It is clear that the low-field component collapses much faster than the high-field one, and that it is essentially gone by 60 K. However, there is no feature in the χ_{ac} data associated with this collapse (see Fig. 3). The transition observed by χ_{ac} clearly reflects the later loss of the high-field component near 100 K. Examination of the 80-K spectrum shows

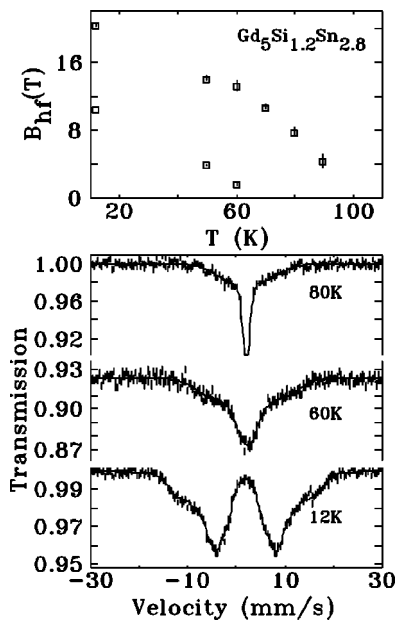


FIG. 9. Bottom: ^{119}Sn Mössbauer spectra of $\text{Gd}_5\text{Si}_{1.2}\text{Sn}_{2.8}$ at several temperatures. This sample only shows the two Gaussian-broadened sextets. Top: Temperature dependence of the average hyperfine fields for the two Gaussian-broadened components.

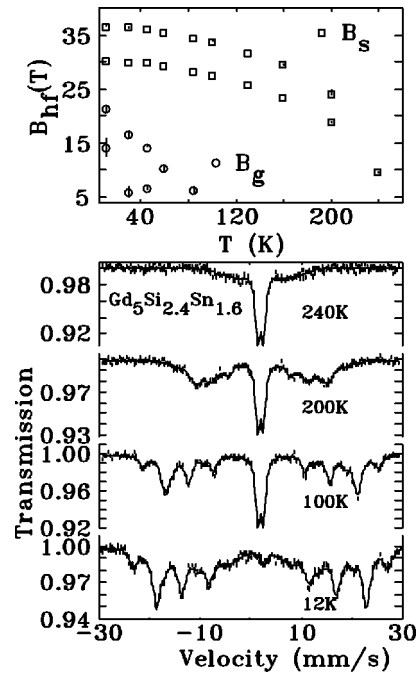


FIG. 10. Bottom: ^{119}Sn Mössbauer spectra of $\text{Gd}_5\text{Si}_{1.6}\text{Sn}_{2.4}$ at several temperatures. This sample shows both the sharp and the Gaussian-broadened sextets. Top: Temperature dependence of the average hyperfine fields for the sharp (B_s) and Gaussian-broadened (B_g) components.

that raising the temperature does more than just reduce the magnetic splitting: It also leads to the growth of a central singlet. Indeed, all of the samples that exhibited a Gaussian broadened component in their 12-K spectra showed this development of the central singlet at the expense of the broad component with increasing temperature. Furthermore, where a singlet component was observed at 12 K, it was possible to eliminate it almost entirely by cooling to 5 K. We therefore attribute the singlet to the same disordered phase that gives the two Gaussian broadened sextets. It is likely that the gradual evolution from sextet to singlet on heating reflects the severe atomic and magnetic disorder present in this phase. The extensive disorder may permit a range of stoichiometries to be present in any given sample, leading to a wide range of effective ordering temperatures. The transition temperature determined by χ_{ac} then reflects the highest ordering temperature present.

On the Si-rich side of the monoclinic phase ($x>1.6$), the spectra are dominated by the two sharp sextets from the orthorhombic phase. With increasing temperature, the spectra (Fig. 10) show the growth of a central feature as the disordered monoclinic phase gradually passes through its ordering region. The splitting of the two sharp sextets is reduced steadily as T_c for the orthorhombic phase is approached, and the pattern collapses in a conventional manner at T_c .

By contrast, the behavior of the Sn-rich orthorhombic phase ($x<0.8$) is strikingly different. Figure 11 shows the temperature dependence of the spectra for Gd_5Sn_4 . As with the other compositions, the central feature grows as the disordered phase is gradually heated through its T_c range, while the fields at the two sites from the orthorhombic phase de-

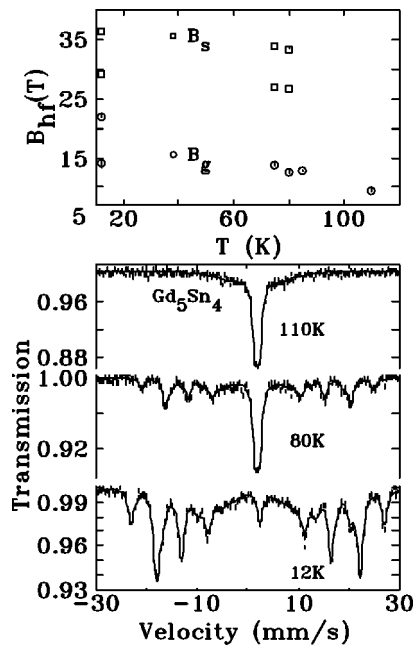


FIG. 11. Bottom: ^{119}Sn Mössbauer spectra of Gd_5Sn_4 at several temperatures. This sample shows an abrupt transition to a nonmagnetic state at 80 K as the sharp sextets disappear. Top: Temperature dependence of the hyperfine fields for the sharp (B_s) and Gaussian-broadened (B_g) components. The sharp sextets are lost between 80 and 85 K.

cline slowly. However, on passing through 80 K the sharp components vanish abruptly. At 80 K, the fields are 34 and 27 T, but by 85 K only a broad feature with an average field of 13 T remains. This broad magnetic component declines gradually on further heating and is lost by ~ 140 K, accounting for the weak pedestal seen in the χ_{ac} data for this alloy (Fig. 3). The abrupt collapse of the two sharp magnetic sextets is likely due to a first-order structural transition from a ferromagnetic phase to a nonmagnetic phase at ~ 85 K. Similar behavior has been reported in the related

$\text{Gd}_5\text{Si}_x\text{Ge}_{4-x}$ alloy system where a first-order structural transition between two ferromagnetic phases has been observed.^{3,5} The two phases have been identified as being closely related orthorhombic structures for $\text{Gd}_5\text{Si}_{0.4}\text{Ge}_{3.6}$,¹² and an orthorhombic to monoclinic distortion occurs for $\text{Gd}_5\text{Si}_2\text{Ge}_2$.¹³ Since the structural transformation in the $\text{Gd}_5\text{Si}_x\text{Ge}_{4-x}$ system was associated with a giant magnetocaloric effect,³ it would seem reasonable to expect the same behavior to be present in the Sn-rich $\text{Gd}_5\text{Si}_x\text{Sn}_{4-x}$ alloys. Finally, the coupled magnetic and structural transformation observed at 85 K in Gd_5Sn_4 explains the contradiction between the single-phased behavior observed (at room temperature) by x-ray diffraction, and the clearly multiphased Mössbauer spectrum at 12 K.

VI. CONCLUSIONS

The ternary alloy system $\text{Gd}_5\text{Si}_x\text{Sn}_{4-x}$ forms for all x . At the Sn-rich and Sn-poor ends, we observe a $Pnma$ orthorhombic Sm_5Sn_4 -type structure. A disordered monoclinic phase is observed for $x \sim 1$. The orthorhombic phases are strongly ferromagnetic with ordering temperatures that decline with increasing tin concentrations. By contrast, the transition temperature of the monoclinic phase is composition independent, but likely exhibits noncollinear magnetic order. ^{119}Sn Mössbauer spectroscopy shows remarkably large transferred hyperfine fields (approaching 37 T) at the Sn sites in the orthorhombic phases. We found clear evidence for a first-order, magnetic, and structural transformation at around 85 K for $x \leq 0.4$. This transition is expected to be associated with a giant magnetocaloric effect.

ACKNOWLEDGMENTS

This work was supported by grants from the Natural Sciences and Engineering Research Council of Canada and Fonds pour la formation de chercheurs et l'aide à la recherche, Québec.

¹G.S. Smith, Q. Johnson, and A.G. Tharp, *Acta Crystallogr.* **22**, 269 (1967).

²F. Holtzberg, R.J. Gambino, and T.R. McGuire, *J. Phys. Chem. Solids* **28**, 2283 (1967).

³V.K. Pecharsky and K.A. Gschneidner, Jr., *Phys. Rev. Lett.* **78**, 4494 (1997).

⁴V.K. Pecharsky and K.A. Gschneidner, Jr., *J. Alloys Compd.* **260**, 98 (1997).

⁵V.K. Pecharsky and K.A. Gschneidner, Jr., *Appl. Phys. Lett.* **70**, 3299 (1997).

⁶K.A. Gschneidner, Jr., V.K. Pecharsky, A.O. Pecharsky, V.V. Ivchenko, and E.M. Levin, *J. Alloys Compd.* **303**, 214 (2000).

⁷H.F. Yang, G.H. Rao, G.Y. Liu, Z.W. Quyang, W.F. Liu, X.M.

Feng, W.G. Chu, and J.K. Liang, *J. Alloys Compd.* **346**, 190 (2002).

⁸H.B. Wang, Miryam Elouneq-Jamróz, D.H. Ryan, and Z. Altounian, *J. Appl. Phys.* (to be published).

⁹L. Morellon, P.A. Algarabel, M.R. Ibarra, J. Blasco, and B. Garcia-Landa, *Phys. Rev. B* **58**, R14 721 (1998).

¹⁰A.C. Larson and R.B. von Dreele, GSAS Report No. LAUR 86-748, 1994 (unpublished).

¹¹D. Ravot, A. Percheron-Guegan, J. Jove, J.L. Dormann, and O. Gorochov, *Soc. Italiana di Fisica* **50**, 363 (1996).

¹²L. Morellon, J. Blasco, P.A. Algarabel, and M.R. Ibarra, *Phys. Rev. B* **62**, 1022 (2000).

¹³W. Choe, V.K. Pecharsky, A.O. Pecharsky, K.A. Gschneidner, Jr., V.G. Young, Jr., and G.J. Miller, *Phys. Rev. Lett.* **84**, 4617 (2000).